

Original Research

Kaempferol Alleviates Injury in Human Retinal Pigment Epithelial Cells via STAT1 Ubiquitination-Mediated Degradation of IRF7

Hongjun Zhang¹, Can Liu¹, Cao Gu², Jun Jiang³, Yu Gao^{4,*}

Academic Editor: Dario Rusciano

Submitted: 26 October 2023 Revised: 26 January 2024 Accepted: 22 March 2024 Published: 4 July 2024

Abstract

Background: Retinal pigment epithelial (RPE) cells have a pivotal function in preserving the equilibrium of the retina and moderating the immunological interaction between the choroid and the retina. This study primarily focuses on delineating the protective effect offered by Kaempferol (Kae) against RPE cell damage. **Methods**: Bioinformatics analysis was performed on the GSE30719 dataset to identify hub genes associated with RPE. Subsequently, we analyzed the impact of Kae on RPE apoptosis, cell viability, and inflammatory response through cell experiments, and explored the interaction between hub genes and Kae. **Results**: Based on the GSE30719 dataset, nine hub genes (*ISG15*, *IFIT1*, *IFIT3*, *STAT1*, *OASL*, *RSAD2*, *IRF7*, *MX2*, and *MX1*) were identified, all of which were highly expressed in the GSE30719 case group. Kae could boost the proliferative activity of RPE cells caused by lipopolysaccharide (LPS), as well as reduce apoptosis and the generation of inflammatory factors (tumor necrosis factor receptor (TNFR), interleukin-1beta (IL-1β)) and cytokines (IL-1, IL-6, IL-12). *STAT1* was shown to inhibit cell proliferation, promote apoptosis, and secrete IL-1/IL-6/IL-12 in LPS-induced RPE cells. Moreover, *IRF7* was found to interact with *STAT1* in LPS-induced RPE cells, and STAT1 could maintain IRF7 levels through deubiquitination. In addition, we also found that the protective effect of Kae on LPS-induced RPE cell injury was mediated through *STAT1/IRF7* axis. **Conclusion**: This study provided evidence that Kae protects RPE cells via regulating the *STAT1/IRF7* signaling pathways, indicating its potential therapeutic relevance in the diagnosis and management of retinal disorders linked with RPE cell damage.

Keywords: retinal pigment epithelium; kaempferol; STAT1; IRF7; ubiquitination

1. Background

A specialized group of cells, known as Retinal pigment epithelial (RPE) cells, are strategically situated in the retina's outermost layer [1]. These cells play an indispensable role in the upkeep and operational efficiency of photoreceptors-the vision-enabling, light-sensitive cells [2]. The blood-retinal barrier, which prevents harmful substances from entering the retina, is maintained by the RPE, a single layer of pigmented cells that performs a variety of vital tasks [3,4]. These include the transport of nutrients, the phagocytosis of shed photoreceptor outer segments, and waste products, and the transport of nutrients [5]. Various retinal degenerative diseases including Stargardt disease, retinitis pigmentosa, and age-related macular degeneration are associated with the dysfunction or depletion of RPE cells [6,7]. Such conditions can culminate in severe visual impairment or even total loss of sight [8]. Therefore, research on RPE cells is crucial for understanding the pathogenesis of these diseases and developing effective therapeutic strategies.

As a naturally occurring flavonoid, Kaempferol (Kae) has attracted significant attention within the scientific community [9]. This is attributed to its broad spectrum of bi-

ological effects encompassing not only anti-cancer properties, and anti-inflammatory capabilities, but also antioxidant [10,11]. In relation to RPE cells, Kaempferol has surfaced as a prospective compound in preempting and addressing the deterioration associated with retinal disorders, exemplified by retinitis pigmentosa and age-related macular degeneration [12,13]. Kaempferol protects RPE cells, according to recent study, by altering a number of signaling pathways related to inflammation, apoptotic cell death and others [13]. The study showed that the tissue factor-targeting peptide (TF-TP) inhibited lipopolysaccharide (LPS)-induced proliferation of ARPE-19 cells and maintained RPE tight junctions by inhibiting TF and increasing ZO-1 expression [14]. Furthermore, Kaempferol was shown to promote the survival and function of RPE cells under different stress conditions, which may be crucial for delaying or reversing the progression of retinal degenerative diseases [15]. The investigation of Kae's impact on RPE cells represents an area of active research, with the potential to reveal novel therapeutic targets and strategies for the management of retinal disorders.

The goal of this research is to investigate the role of Kae in regulating RPE cell activities, including LPS-

¹Department of Ophthalmology, Minhang Hospital, Fudan University, 201100 Shanghai, China

²Department of Ophthalmology, Xinshijie Zhongxing Eye Hospital, 200050 Shanghai, China

³Endoscopy Center, Minhang Hospital, Fudan University, 201100 Shanghai, China

⁴Department of Ophthalmology, Changhai Hospital Affiliated to Navy Medical University, 200433 Shanghai, China

^{*}Correspondence: gaoyu@smmu.edu.cn (Yu Gao)

induced proliferation, apoptosis, and inflammatory cytokine release. First, we used bioinformatics approaches to identify hub genes that are directly associated to RPE cells in public databases. Following that, the effect of Kae on RPE cell damage was explored *in vitro* using a variety of cell studies. The findings of this research will bring new ideas for prospective treatment techniques for RPE injury and inflammation in ocular illnesses.

2. Material and Methods

2.1 Gene Expression Omnibus (GEO) for Weighted Gene Co-Expression Network Analysis (WGCNA)

We searched the GEO with the keyword "RPE cells", "West Nile Virus (WNV)", and identified the GSE30719 dataset. Based on the "WGCNA" package (version 4.1.0) of the R software (version 4.1.0, https://www.r-project.org/), we constructed a gene co-expression network for all genes in the GSE30719 dataset, and determined the optimal soft threshold to make the network conform to a scale-free topology. Then, the dissimilarity coefficient of various nodes was determined in accordance with the adjacency function the gene network formed, and a hierarchical clustering tree was created to obtain gene modules of different colors. Subsequently, the correlation between the gene modules and the GSE30719 data sample station was calculated, and a heat map was drawn to screen out the key module.

2.2 The Identification of GSE30719-Differentially Expressed Genes (DEGs)

The GSE30719 dataset (https://www.ncbi.nlm.nih.g ov/geo/query/acc.cgi?acc=GSE30719) includes 10 samples, of which four uninfected RPE cell samples were regarded as the control group, and 4 RPE cells infected with immunopathogenic West Nile virus (WNV) as the case group. Through the GEO2R tool in the GEO database, the up- and down-regulated DEGs in these samples were screened with the standards of fold change (FC) above 1.5 or below 0.67, with a *p*-value less than 0.05.

2.3 Functional Enrichment Analysis on Intersecting Genes

We applied the "ggvenn" package (version 0.1.9) of R software to draw the Venn diagram of brown module and GSE30719-DEGs to identify the intersection genes. Following this, we employed the 'Cluster Profiler' package (version 4.0.1) to perform enrichment analysis, utilizing both the Kyoto Encyclopedia of Genes and Genomes (KEGG) pathways and Gene Ontology (GO) terms. This analysis was conducted on the identified genes with the goal of illuminating their biological attributes. When p < 0.05, the obtained results were significant in statistics.

2.4 Identification of Hub Genes

Subsequently, we inputted the sequence data of the intersecting genes into the Search Tool for the Retrieval of

Interacting Genes (STRING) database. To illustrate the interconnections among these genes, we used Cytoscape software (version 3.8.1, http://www.cytoscape.org/) to construct a visual representation of the protein-protein interaction (PPI) network. Cytohubba is a plugin for Cytoscape that ranks nodes according to their properties in the network, including 11 topological algorithms. Herein, we construct two sub-networks based on the Degree and Maximal Clique Centrality (MCC) algorithms, respectively, and the top 15 genes by each algorithm were displayed. The hub genes were demonstrated through Venn diagram based on the "ggvenn" package.

2.5 Pathway Enrichment of Hub Genes in WNV Infection

The "ggplot2" package (version 3.3.3) of the R software was employed to detect the expressions of nine hub genes in the two groups of the GSE30719 dataset to evaluate whether the gene expression was affected by WNV infection. Subsequently, we delved deeper into the biological attributes of these genes. The KEGG pathway enrichment analysis via Gene Set Enrichment Analysis (GSEA) was performed on these nine genes, and the top four enriched pathways with p < 0.05 for each gene were displayed. These signaling pathways might be involved in the molecular mechanism between these genes and WNV infection in RPE.

2.6 Chemical Structure of Kae

Kae, a flavonoid compound, has the molecular formula $C_{15}H_{10}O_6$ and weighs 286.24 g/mol, was purchased from Wuhan Comic Biomedical Technology Co., Ltd (Wuhan, China). Materials related to cell culture in this experiment were provided by Wuhan Boster Bioengineering Co., Ltd (Wuhan, China).

2.7 Cell Culture, Treatment and Transfection

We cultured RPE cells in DMEM, complemented with 10% FBS and 1% penicillin-streptomycin, maintaining the environment at 37 °C with 5% CO₂. All cell lines were validated by Short Tandem Repeat (STR) profiling and tested negative for mycoplasma. Cells were all cultured in a humidified incubator at 37 °C and 5% CO₂. We then introduced LPS into the culture at 5 µg/mL for a 6-hour period, and concurrently initiated pre-treatment with varying concentrations of Kae (0, 5, 10, 25/50 µmol/L) for 24 hours. We proceeded with further exposure to LPS (5 μg/mL) for another 6 hours, which was followed by transfection using Lipofectamine 2000 to introduce pcDNA3.1-STAT1 or pcDNA3.1-IRF7 plasmids into the cells, as per the protocol provided by the manufacturer. Post-transfection, the cells were subjected to an additional 24 hours incubation in the presence of LPS (5 µg/mL).



2.8 Cell Counting Kit-8 (CCK-8) Assay

Cells were first exposed to LPS at a concentration of 5 μ g/mL for a period of 6 hours to initiate inflammation. This was followed by a 24 hours pre-treatment phase with a range of Kae concentrations (0, 5, 10, 25, or 50 μ mol/L). Subsequent to pre-treatment, cells were introduced to the Cell Counting Kit-8 (CCK-8) reagent. Optical density (OD) measurements were carried out at a wavelength of 450 nm via a microplate reader (BioTek, Shanghai, China).

2.9 Flow Cytometry

Flow cytometry was used to assess RPE cell apoptosis. Cells were pre-treated with Kaempferol (0, 5, or 10 μ mol/L) for 24 hours after being treated with LPS (5 μ g/mL) for 6 hours. Flow cytometry was used to evaluate cells labeled with Annexin V-FITC and propidium iodide (PI).

2.10 Western Blotting (WB) Assay

RPE cells were collected and lysed with RIPA buffer after treatment. A bicinchoninic acid (BCA) assay was used to quantify protein concentrations. Sodium dodecyl-sulfate polyacrylamide gel electrophoresis (SDS-PAGE) was used to separate equal quantities of protein, which was then transferred to polyvinylidene difluoride (PVDF) membranes. After blocking with 5% skimmed milk, the membranes were treated with primary antibodies against apoptotic proteins (cleaved caspase-3 and Bcl-2), STAT1, and IRF7, followed by secondary antibodies conjugated to horseradish peroxidase. Enhanced chemiluminescence (ECL) reagents were used to view protein bands. The intensity was measured using ImageJ software (version 1.53s, LOCI, University of Wisconsin, Madison, WI, USA).

2.11 Quantitative Real-Time Polymerase Chain Reaction (qRT-PCR) Assay

We utilized TRIzol reagent for total RNA extraction from RPE cells, which was subsequently subjected to reverse transcription using PrimeScript RT kit (TaKaRa, Dalian, China). To quantify these expressions, we leveraged an Applied Biosystems 7500 Fast Real Time PCR System (Thermo Fisher Scientific, Waltham, MA, USA) with SYBR Green Master Mix for qRT-PCR. Primers for amplification of IL-1 β , TNFR, STAT1, IRF7 and GAPDH (internal reference) were designed using Primer3 software (version 4.1.0, https://bioinfo.ut.ee/primer3/). The following primers were used for gene expression analysis, IL-1 β forward: 5'-GTACCTGTCCTGCGTGTTGA-3', reverse: 5'-GGGAACTGGGCAGACTCAAA-3'; TNFR forward: 5'-GCCAGGAGGTTTACCTACTG-3', re-5'-GTAGACACTTGCCAGCCATT-3'; STAT1 verse: 5'-GATCAGCTGCAAACGTGGTTC-3', reforward: verse: 5'-GCTTTTTAAGCTGCTGACGGA-3'; IRF7 5'-GCCGAAGTGAGGTGAGAACA-3', reforward: verse: 5'-TATGG CCCTCCTCACCAGTT-3'; GAPDH forward: 5'-ATGACATCAAGAAGGTGGTG-3', reverse:

5'-CATACCAGGAAATGAGCTTG-3'. The $2^{-\Delta \Delta Ct}$ technique was used to calculate relative gene expression levels.

2.12 Enzyme-Linked Immunosorbent Assay (ELISA)

The ELISA kits supplied by Abcam, Cambridge, UK, were employed to quantify the secretion of cytokines IL-1, IL-6 and IL-12 in RPE cell culture supernatant. Cells underwent treatment with 5 μ g/mL LPS for 6 hours and received pre-treatment with Kae at concentrations of 0 or 10 μ mol/L for 24 hours period. Subsequent to this, the culture medium was gathered, centrifuged at 1000 rpm for 10 minutes to eliminate cell remnants, and diluted in a 1:2 ratio with the diluent included in the kit. Following the manufacturer's protocol, the assay was performed, and absorbance was gauged at 450 nm using a Bio-Rad microplate reader, Hercules, CA, USA.

2.13 HitPredict Database

In this study, we utilized the HitPredict database (http://www.hitpredict.org/), an integrative bioinformatics platform that predicts PPI based on experimental evidence and a confidence score system. The database offers a comprehensive collection of PPI derived from multiple sources, including high-throughput experiments and literature-curated data, to facilitate the identification of potential interactions between proteins of interest. To investigate the proteins associated with STAT1, we conducted a search using the Hit-Predict database to identify potential binding partners.

2.14 Co-Immunoprecipitation (Co-IP) Assay

Co-IP was used to identify the interaction between STAT1 and IRF7. Following a pre-treatment with Kae (0 or 10 μ mol/L) for 24 hours, cells were treated with LPS (5 μ g/mL) for 6 hours. Protein A/G beads were used after total protein had been isolated and treated with certain primary antibodies. The immunoprecipitated proteins were analyzed by WB.

2.15 Glutathione S-Transferase (GST) Pull-Down Assay

The aforementioned plasmids were collectively transfected into RPE cells using Lipofectamine 3000 following the provider's protocols. Post-transfection (48 hours), cell collection and lysis took place. Subsequently, the cell lysate underwent a 2-hour incubation with GST beads at 4 °C, ensuring gentle rotation. After a trio of washes with buffer, proteins adhered to the beads were eluted through boiling with SDS-PAGE loading buffer. Following separation via SDS-PAGE, these proteins were transferred onto PVDF membranes. The membranes were then targeted with both anti-Myc and anti-GST antibodies, and further incubated with an HRP-linked secondary antibody. Visualization of protein bands was achieved with a chemiluminescence detection system (Perkin Elmer, Boston, MA, USA).



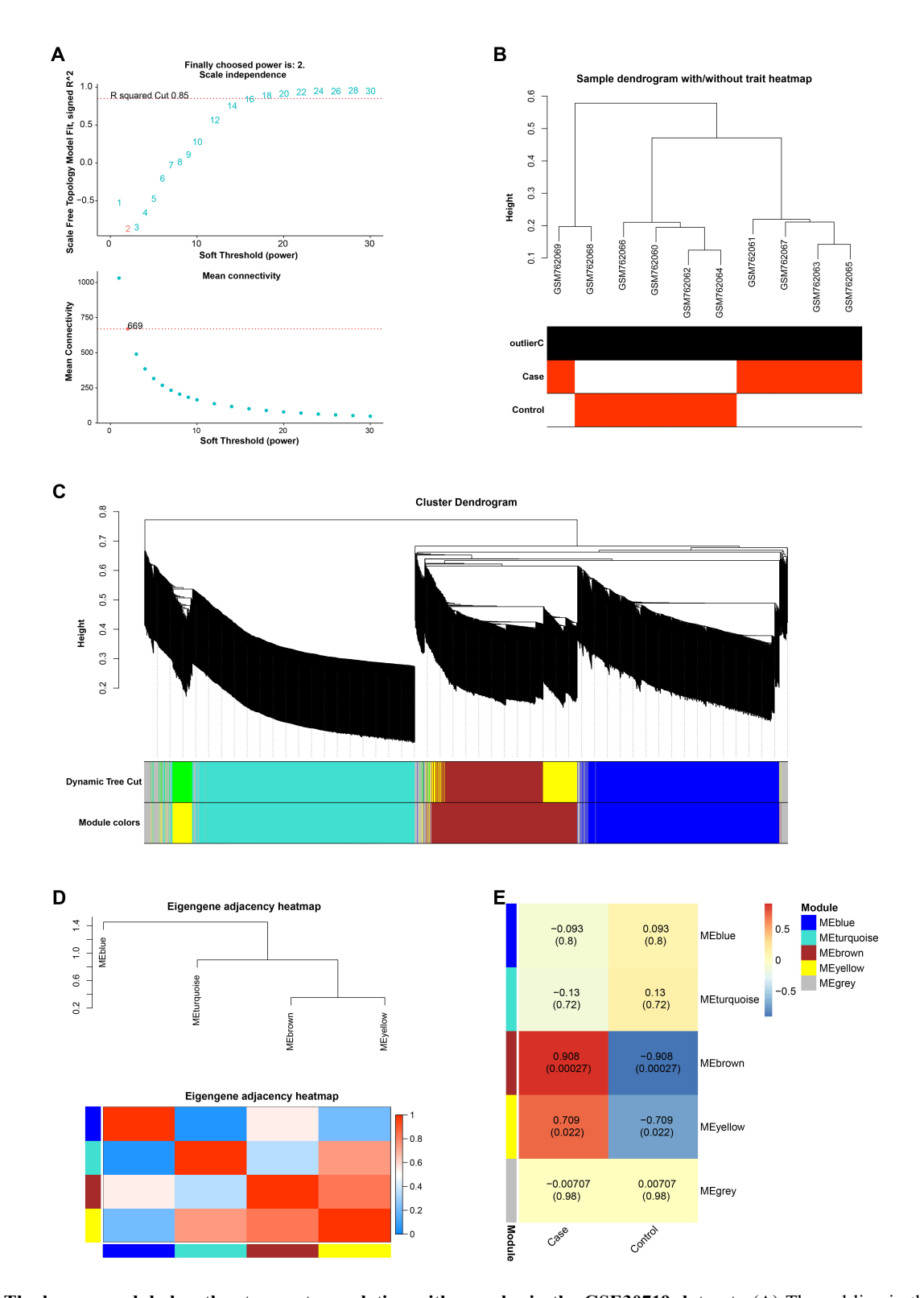


Fig. 1. The brown module has the strongest correlation with samples in the GSE30719 dataset. (A) The red line in the upper figure represents the subjectively selected scale-free fitting index value, 2 is the optimal soft threshold, and the lower figure is the mean connectivity of different soft thresholds. (B) Dendrogram of 10 samples in GSE30719 dataset, different branches represent different samples. (C) The Cluster Dendrogram of the gene module, the upper layer is the hierarchical clustering dendrogram of genes, and the lower layer is the gene modules of different colors. (D) The eigengene adjacency heatmap of gene modules, the different branches above represent different gene modules, and the bottom is the heatmap between gene modules. (E) Heatmap of the correlation between the gene modules and the case and the control groups in the GSE30719 dataset, the larger the correlation coefficient, the stronger the correlation between the module and the sample.

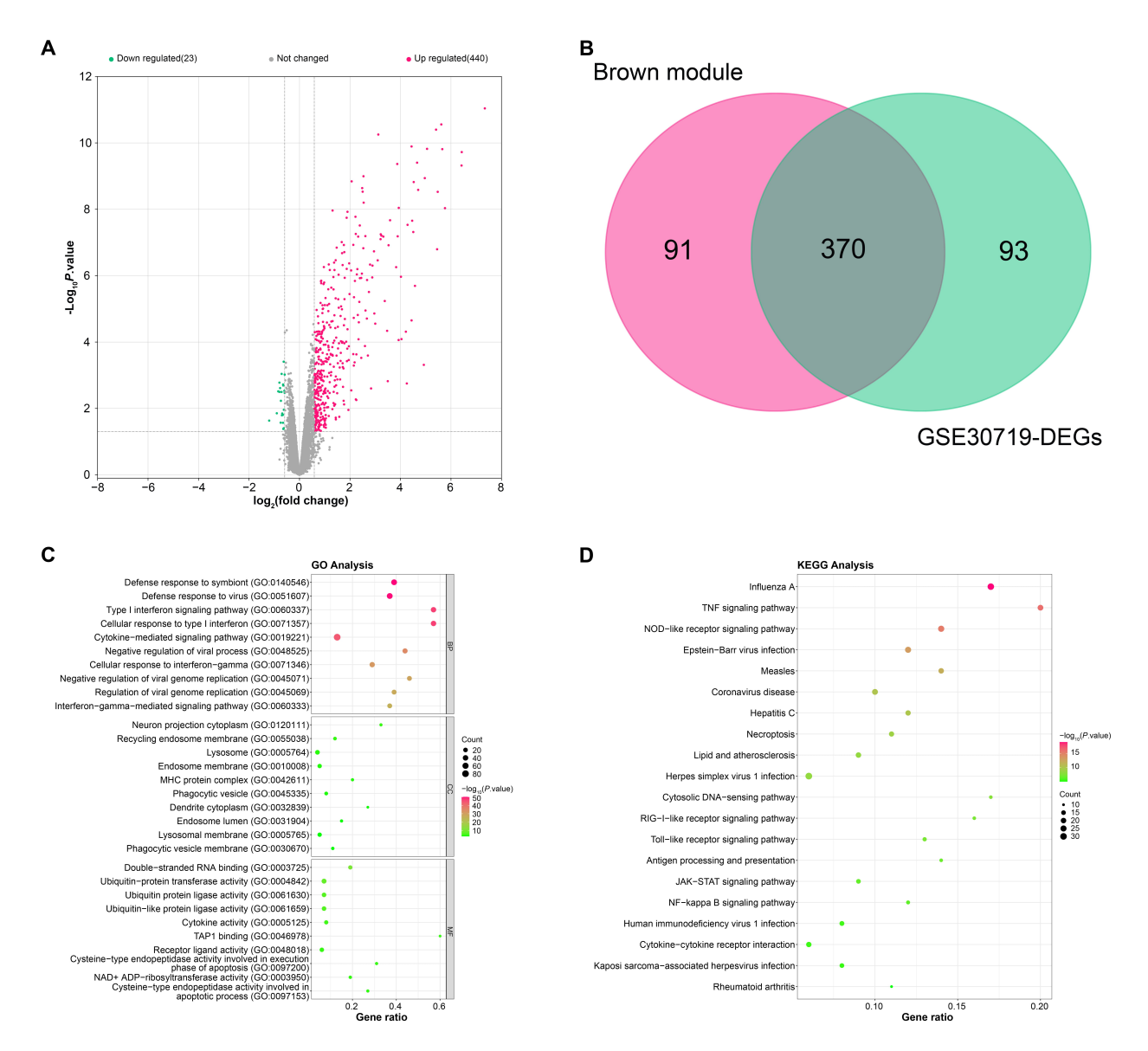


Fig. 2. The intersecting genes from brown module and GSE30719-differentially expressed genes (DEGs). (A) Volcano plot of GSE30719-DEGs, the green scatter on the left represents down-regulated DEGs, and the three red dots on the right represent up-regulated DEGs. (B) The intersecting genes identified from key module and GSE30719 dataset. (C) The enriched Gene Ontology (GO) terms of intersecting genes in biological process (BP), cellular component (CC), molecular function (MF). (D) Top 10 Kyoto Encyclopedia of Genes and Genomes (KEGG) enrichment pathways of intersecting genes.

3. Results

3.1 The Brown Module Has the Strongest Correlation with Samples in the GSE30719 Dataset

The gene co-expression network was constructed for all the genes in the GSE30719 data set by the WGCNA algorithm, and the optimal soft threshold of the network was selected as 2 (Fig. 1A,B). After that, we divided these genes into 4 modules (except the grey module), namely the blue, turquoise, brown and yellow modules, and constructed a cluster dendrogram and eigengene adjacency heatmap (Fig. 1C,D). Subsequently, by comparing the correlations between these gene modules and the control and case groups in the GSE30719 dataset, it was identified that

the brown module had the strongest correlation with strict inability, with a correlation coefficient of 0.908 (Fig. 1E).

3.2 The Intersecting Genes from Brown Module and GSE30719-DEGs

Through the GEO2R tool and screening conditions, we identified 440 up-regulated and 23 down-regulated DEGs from GSE30719, as demonstrated in the volcano plot of Fig. 2A. Based on the "ggvenn" package, we drew a Venn diagram of brown module and GSE30719-DEGs, from which 370 intersecting genes were identified (Fig. 2B). In the GO analysis on the intersecting genes, it was found that these genes were enriched in Defense re-



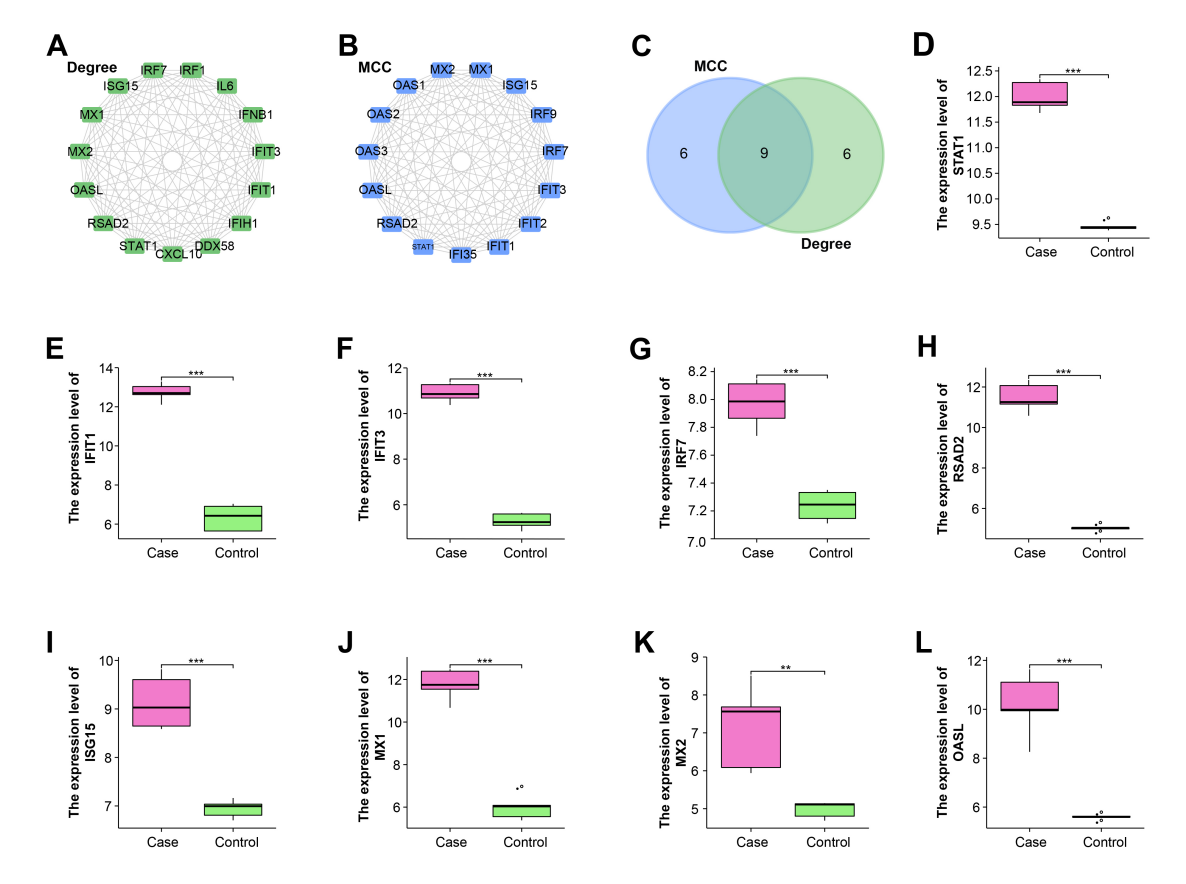


Fig. 3. Nine hub genes are identified from protein-protein interaction (PPI) sub-networks. (A) The sub-network of the top 15 genes constructed by the Degree algorithm. (B) The sub-network of the top 15 genes constructed by the Maximal Clique Centrality (MCC) algorithm. (C) Nine hub genes identified from genes in Degree and MCC algorithms. (D–L) Hub genes are all highly expressed in the case group of GSE30719 dataset, including (D) STATI. (E) IFITI. (F) IFITI3. (G) IRFT7. (H) RSAD2. (I) ISGI55. (J) MXI7. (K) MX27. (L) OASL8. **P9 < 0.01, ***P9 < 0.001.

sponse to symbiont, Cytokine-mediated signaling pathway, Defense response to virus, etc. (biological process, BP), MHC protein complex, Endosome membrane, Lysosome, Recycling endosome membrane, Neuron projection cytoplasm, etc. (Fig. 2C, cell component), Cytokine activity, Double-stranded RNA binding and so on (molecular function). Besides, these genes were related to KEGG pathways like Coronavirus disease, Measles, Influenza A (Fig. 2D).

3.3 Nine Hub Genes are Identified from PPI Sub-Networks

Next, the sub-networks of intersecting genes were constructed through the Degree and MCC algorithms of the Cytohubba plugin (Fig. 3A,B). Then by Venn diagram, nine hub genes related to WNV infection in RPE were identified, namely *ISG15*, *IFIT1*, *IFIT3*, *STAT1*, *OASL*, *RSAD2*, *IRF7*, *MX2*, and *MX1* (Fig. 3C).

3.4 Hub Genes are All Highly Expressed in the Case Group of GSE30719 Dataset

To explore the expressions of hub genes in PRE cells, we detected the expressions of these genes in the case group and control group of the GSE30719 dataset based on the "ggplot2" package. According to the results in Fig. 3D—

L, it was clearly observed that *IFIT1*, *IFIT3*, *IRF7*, *ISG15*, *MX1*, *MX2*, *OASL*, *RSAD2*, *STAT1* were generally highly expressed in the case group, which indicated they were all related to WNV infection.

3.5 The Enriched KEGG Pathways of Hub Genes by GSEA

Through the GSEA, we performed KEGG pathway enrichment analysis on 9 hub genes, respectively (Fig. 4A–I). For instance, IFIT1 were enriched in Lysine degradation, Propionate metabolism, Butyrate metabolism and PRAR signaling pathway, and IFIT3 were related to Autoimmune thyroid disease, RIG I like receptor signaling pathway, Cytosolic DNA sensing pathway, and Glycosaminoglycan biosynthesis heparan sulfate. These signaling pathways might be involved in the molecular mechanism between these genes and WNV infection in RPE.

3.6 Kae Attenuates the Apoptosis of RPE Cells Induced by LPS

Then, we tested the impact of Kae on RPE cells (Fig. 5A). RPE cells underwent a 6-hour exposure to LPS at a dosage of 5 μ g/mL, followed by pretreatment with var-



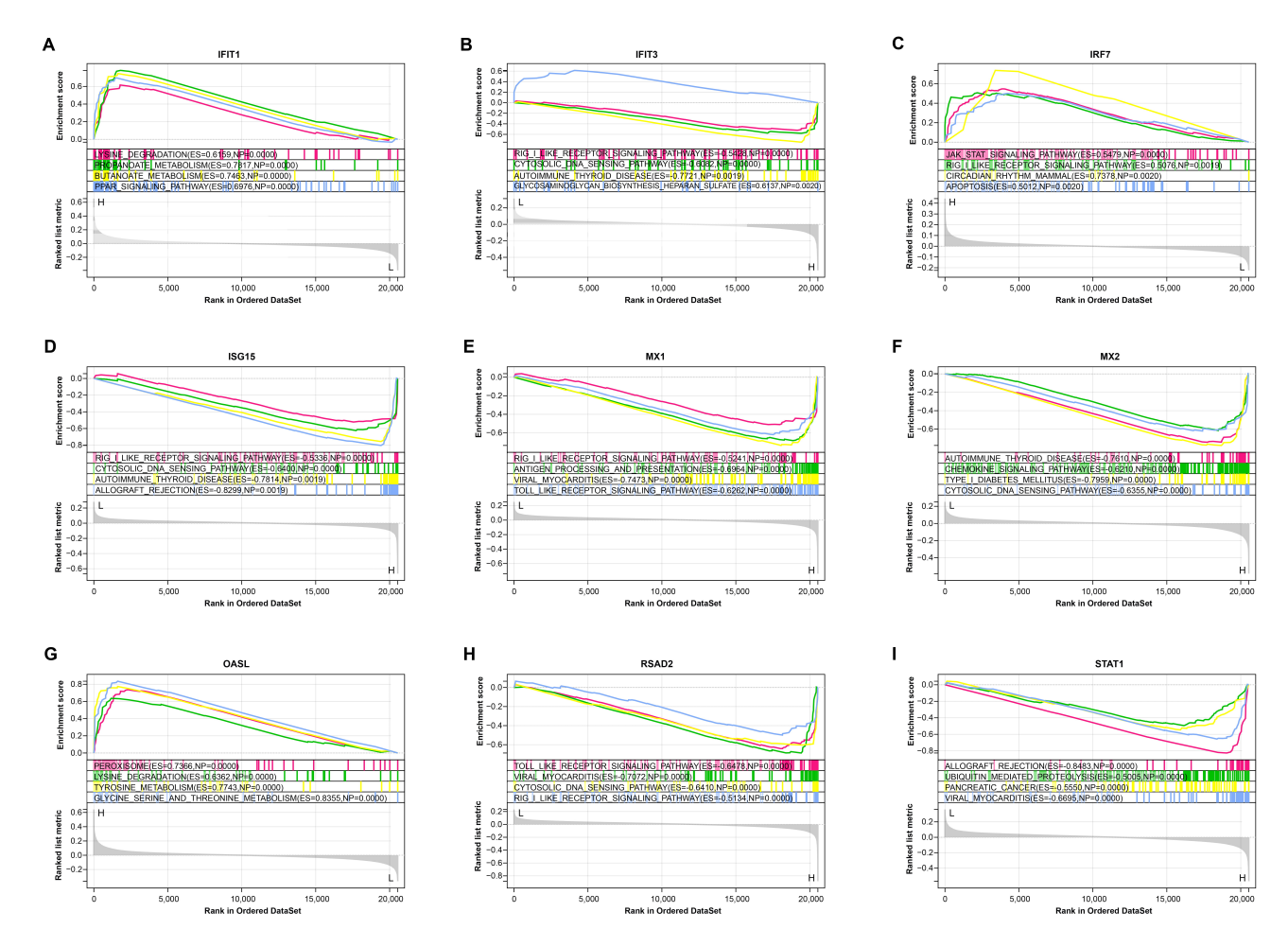


Fig. 4. Gene set enrichment analysis (GSEA)-KEGG pathway enrichment analysis of nine hub genes. (A) *IFIT1*. (B) *IFIT3*. (C) *IRF7*. (D) *ISG15*. (E) *MX1*. (F) *MX2*. (G) *OASL*. (H) *RSAD2*. (I) *STAT1*.

ious concentrations of Kae (0, 5, 10, 25, and 50 μ mol/L) for 24 hours. The maximum cell proliferation viability was reported at 10 μ mol/L Kae in the CCK-8 assay, followed by 5 μ mol/L (Fig. 5B). Flow cytometry analysis indicated a minimal apoptosis rate in cells exposed to 10 μ mol/L Kae, as compared to those treated with a 5 μ mol/L concentration (Fig. 5C,D). Consequently, for next tests, we chose a Kae concentration of 10 μ mol/L as the ideal. Furthermore, WB results showed that the expression of pro-apoptotic protein caspase-3 was down-regulated and the expression of antiapoptotic protein Bcl-2 was up-regulated in Kae-treated RPE cells (Fig. 5E–G). It was concluded that Kaempferol exerted a protective effect against LPS-induced RPE cell apoptosis at the optimal concentration of 10 μ mol/L.

3.7 Kae Attenuates Inflammatory Cytokine Expression and Secretion in LPS-Induced RPE Cells

IL- 1β , TNFR, IL-1, IL-6, and IL-12 are vital for regulating the immune response and are implicated in the pathogenesis of various inflammatory conditions [16]. These cytokines have been reported to be involved in the interaction with RPE cells, influencing cellular processes and contributing to retinal diseases [17]. We used qRT-PCR

to evaluate mRNA levels to study the influence of Kae on the production of these inflammatory cytokines in RPE cells. As shown in Fig. 6A,B, IL- $I\beta$ and TNFR mRNA expression levels in LPS-treated RPE cells were significantly decreased after Kae treatment compared with the control group. Furthermore, ELISA results revealed that Kae also exerted a significant inhibitory effect on IL-1, IL-6 and IL-12 production levels in LPS-treated RPE cells (Fig. 6C–E). Thus, our findings demonstrated that Kae effectively attenuates the expression and secretion of key inflammatory cytokines in LPS-induced RPE cells, highlighting its potential as a therapeutic agent for retinal inflammatory conditions.

3.8 Overexpression of STAT1 Promotes LPS-Induced Apoptosis and Secretion of Inflammatory Cytokines in RPE Cells

STAT1 is a transcription factor that regulates several physiological functions, such inflammation, apoptosis, and immune response [18]. This study pointed out that the identified hub gene might have an effect on the immune response and cell metabolism of RPE cell injury. In this experiment, we observed that after LPS induction of RPE cells, Kae treatment resulted in the downregulation of



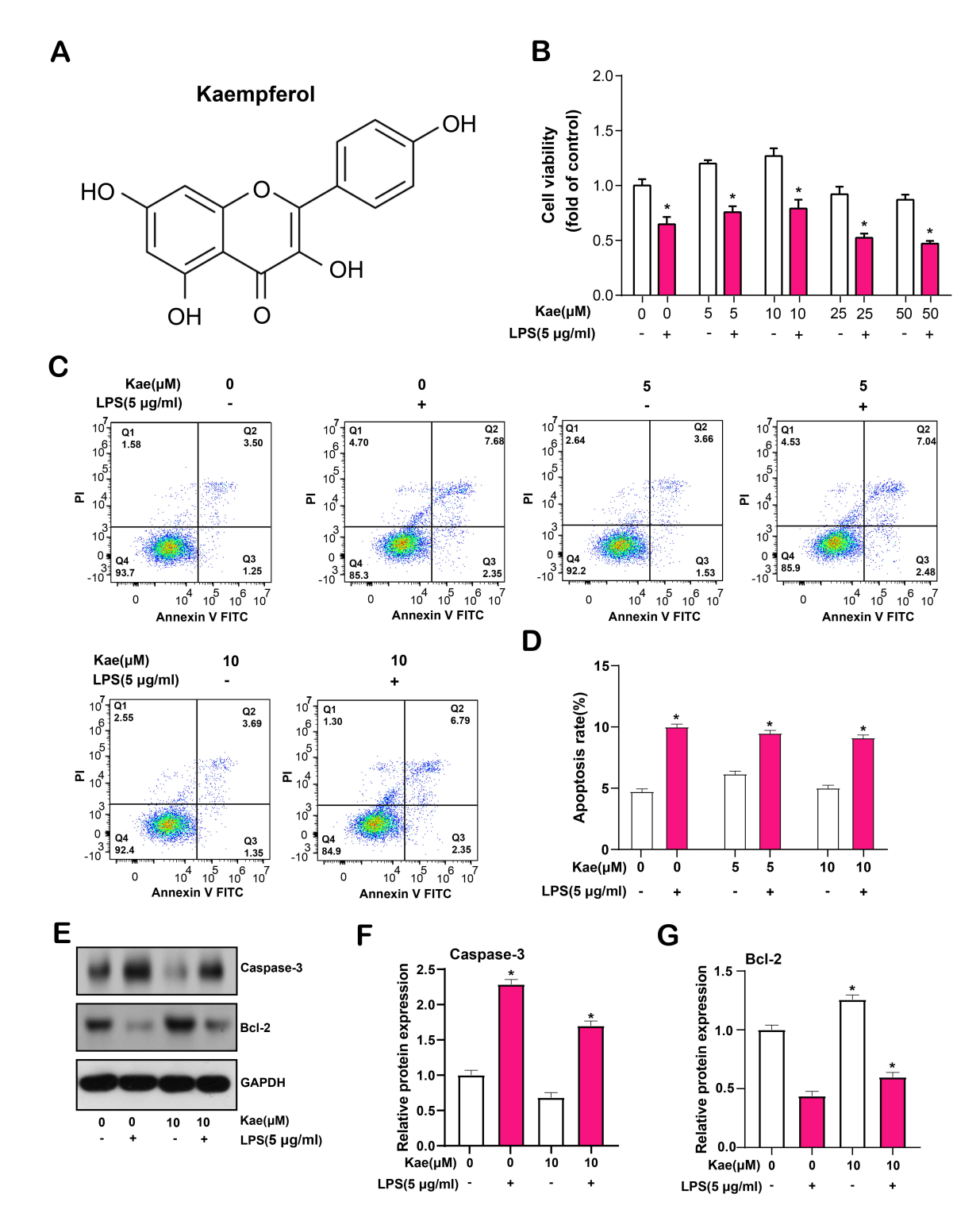


Fig. 5. Kaempferol protects retinal pigment epithelial (RPE) cells from lipopolysaccharide (LPS)-induced apoptosis. (A) Chemical structural formula of kaempferol. (B) Cell Counting Kit-8 (CCK-8) was used to detect the effect of different concentrations of Kae on the proliferation of RPE cells induced by LPS for 6 hours. (C,D) Flow cytometry comparing the apoptosis rate of RPE cells treated with 5 μ mol/L and 10 μ mol/L Kae, with the lowest apoptosis rate observed at 10 μ mol/L. Quadrant Q1 represents necrotic cells (Annexin V-FITC negative, Propidium Iodide (PI) positive), quadrant Q2 represents late apoptotic cells (Annexin V-FITC positive, PI positive), quadrant Q3 represents early apoptotic cells (Annexin V-FITC positive, PI negative), and quadrant Q4 represents live cells (Annexin V-FITC negative, PI negative). (E–G) Western Blotting (WB) analysis of protein expression levels of cleaved caspase-3 and Bcl-2 in RPE cells treated with Kae, GAPDH as internal reference. The bar graph on the right shows the results of the gray-scale detection of proteins. *p < 0.05.

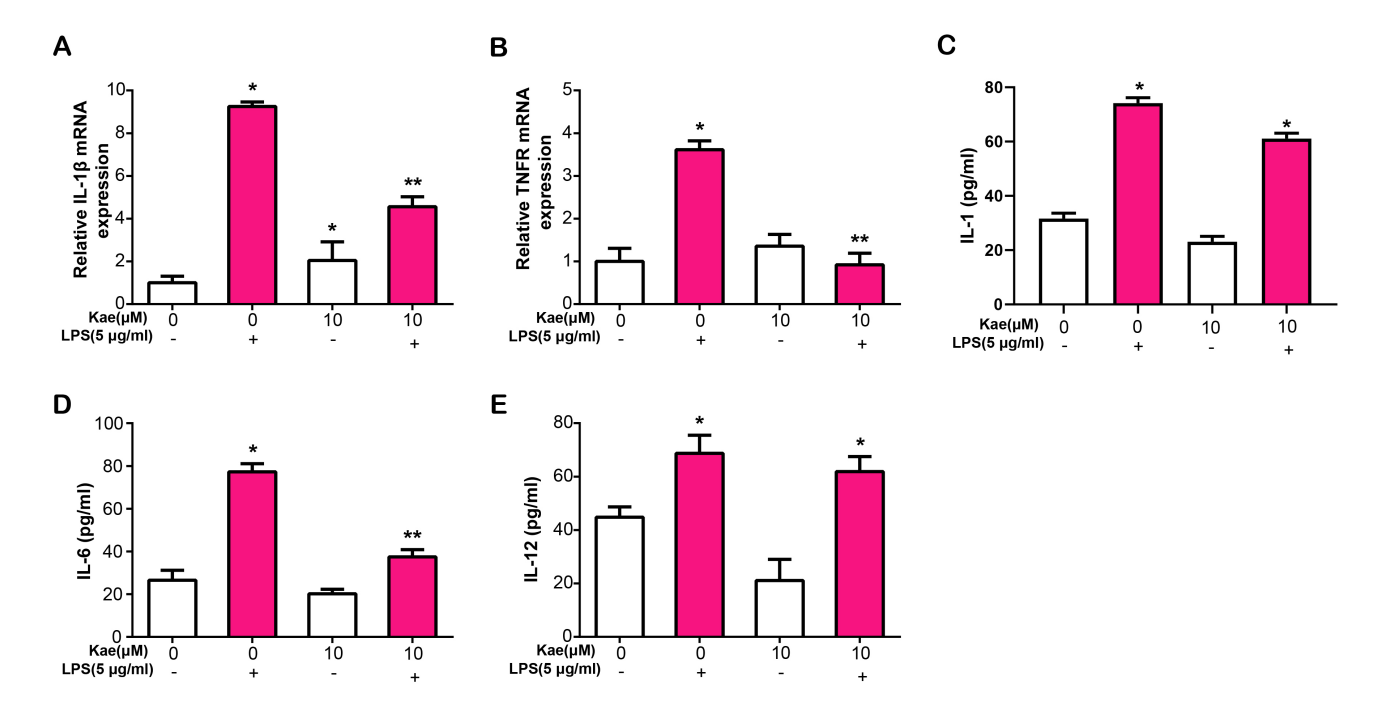


Fig. 6. Kae modulates inflammatory cytokine expression and secretion in LPS-Treated RPE cells. (A) Quantitative real-time polymerase chain reaction (qRT-PCR) analysis of IL- 1β mRNA expression in RPE cells treated with LPS for 6 hours and pretreated with Kae for 24 hours. (B) qRT-PCR analysis of INFR mRNA expression in RPE cells treated with LPS for 6 hours and pretreated with Kae for 24 hours. (C–E) Enzyme-linked immunosorbent assay (ELISA) measurement of IL-1, IL-6 and IL-12 secretion levels in the culture supernatant of RPE cells treated with LPS for 6 hours and pretreated with Kae (0 or 10 μ mol/L) for 24 hours. *p < 0.05, **p < 0.01.

STAT1 mRNA expression (Fig. 7A). Further WB research revealed that LPS and Kae-treated RPE cells had lower STAT1 protein levels (Fig. 7B,C). Subsequently, we overexpressed STAT1 in RPE cells and analyzed the overexpression efficiency using qRT-PCR and WB (Fig. 7D,E). CCK-8 analysis revealed that a significant suppression in LPSinduced RPE cell proliferation with STAT1 overexpression, in comparison to the control (Fig. 7F). In contrast, flow cytometry showed that overexpression of STAT1 promoted LPS-induced apoptosis of RPE cells (Fig. 7G,H). Furthermore, ELISA analysis evaluated the effect of STAT1 overexpression on the release of IL-1, IL-6 and IL-12, three inflammatory cytokines, in LPS-stimulated RPE cells, which unveiled an enhancement in their secretion levels (Fig. 7I-K). This data suggested that STAT1 overexpression has the capacity to modulate LPS-induced RPE cell proliferation, apoptosis and inflammation-related cytokine release.

3.9 STAT1 Have an Interaction with IRF7 in LPS-Treated RPE Cells

By the HitPredict database, we observed 15 proteins with potential interactions with STAT1 (Fig. 8A). *IRF7*, an interferon regulatory factor, not only regulates immune responses and apoptosis, but may also be involved in immune responses in RPE injury. Therefore, in this study, we selected *IRF7* for further verification analysis. qRT-PCR and WB analyses detected that *IRF7* mRNA and protein lev-

els were reduced in RPE cells treated with LPS and Kae (Fig. 8B,C). The link between STAT1 and IRF7 in RPE cells was validated by both exogenous and endogenous Co-IP findings (Fig. 8D,E). Besides, the GST-pull down test findings confirmed the interaction among *STAT1* as well as *IRF7* in RPE cells (Fig. 8F,G).

3.10 Regulatory Mechanism of STAT1 on IRF7 Protein Stability and Ubiquitination in RPE Cells

Further research was done on STAT1 and IRF7's regulation mechanisms in RPE cells. First, we used qRT-PCR to measure the mRNA level of IRF7 in RPE cells following STAT1 overexpression and discovered that it was unaffected (Fig. 9A). However, WB analysis revealed that overexpression of STAT1 significantly upregulated IRF7 protein levels (Fig. 9B). Consequently, we postulated that the regulation of IRF7 by STAT1 at the transcriptional level was unlikely. To validate this hypothesis, we performed CHX chase analysis and MG132 treatment. In STAT1-overexpressing cells treated with CHX, the half-life of IRF7 protein was substantially shortened, indicating that STAT1 was involved in the regulation of IRF7 protein stability (Fig. 9C). Subsequently, we determined whether STAT1 induced the degradation of IRF7 by promoting its ubiquitination in RPE cells. As shown in Fig. 9D, overexpression of STAT1 significantly increased IRF7 ubiquitination levels, thereby promoting the degradation of IRF7.



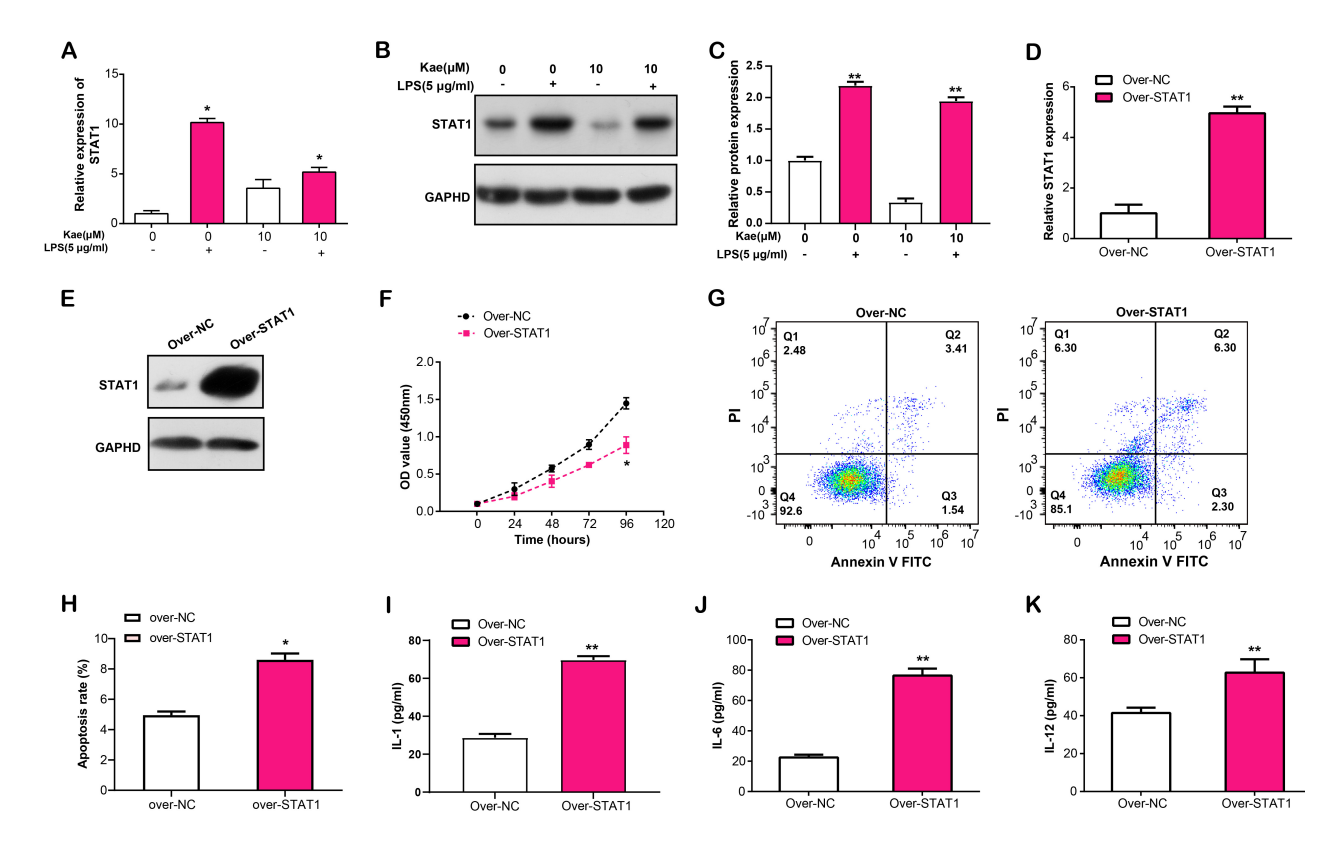


Fig. 7. Effects of STAT1 overexpression on the proliferation, apoptosis, and inflammatory cytokine secretion in LPS-induced RPE cells. (A) qRT-PCR analysis of STAT1 mRNA expression in RPE cells treated with LPS and Kae. (B,C) WB analysis of STAT1 protein levels in RPE cells treated with LPS and Kae. (D) qRT-PCR and (E) WB analysis of STAT1 overexpression efficiency in RPE cells. (F) CCK-8 assay for the effect of STAT1 overexpression on LPS-induced proliferation of RPE cells. (G,H) Flow cytometry analysis of the effect of STAT1 overexpression on LPS-induced RPE cell apoptosis. (I–K) ELISA analysis of IL-1, IL-6 and IL-12 secretion levels in RPE cells with STAT1 overexpression following LPS induction. *p < 0.05, **p < 0.01.

3.11 Kae Attenuates LPS-Induced RPE Cells Injury via STAT1/IRF7 Axis

In the following experiments, we overexpressed IRF7 in LPS-induced RPE cells, confirmed by qRT-PCR and WB assays (Fig. 10A,B). To verify the regulatory effects of overexpressed STAT1 and IRF7 on LPS-induced RPE cells, we divided RPE cells into six groups, namely pcDNA3.1, over-STAT1, over-STAT1 + over-IRF7, pcDNA3.1 + Kae, over-STAT1 + Kae and over-STAT1 + over-IRF7 + Kae. CCK-8 assay revealed that RPE cells treated with Kae exhibited the highest proliferation capacity, while the simultaneous treatment of overexpressed STAT1 or IRF7 resulted in reduced proliferation capacity of RPE cells (Fig. 10C). The flow cytometry results of cell apoptosis showed the highest apoptosis rate in the over-STAT1 + over-IRF7 group, while the apoptosis rate of RPE cells decreased after Kae treatment (Fig. 10D-I). Finally, ELISA results confirmed that STAT1/IRF7 overexpression in LPS-induced RPE cells led to increased IL-1, IL-6 and IL-12 production levels in the cell culture supernatant. Following Kae therapy, IL-1/IL-6/IL-12 secretion levels were downregulated (Fig. 10J–L). Our results implied that Kae alleviates LPS-induced RPE cell injury through the STAT1/IRF7 pathway.

4. Discussion

The RPE consists of a monolayer of RPE cells that are regularly arranged and linked with the choroid by Bruch's membrane [19]. Previous research had found RPE has a significant impact on maintaining visual function and circulation, and it can also phagocytose and reduce shed Photoreceptor Outer Segments (POS), keep visual cell renewal consistent, prevent light damage, and function as a barrier and material transport [20,21]. Bertolotti E et al. [22] thought inherited maculopathy, age-related macular degeneration and retinitis pigmentosa were associated with impaired or loss of RPE function. Zhang D et al. [23] mentioned that atrophic changes in RPE could cause Stargardt disease, which could be prevented by c20d 3-vitamin A. In this paper, we searched for potentially hub genes and biological pathways related to RPE cell injury by GSE30719 dataset.

We constructed a gene co-expression network of all genes in the GSE30719 dataset based on the WGCNA algorithm, and screened out the brown module with the strongest correlation with the samples. After that, we screened the GSE30719-DEGs dataset based on the GEO2R tool, and selected the overlapping genes combined



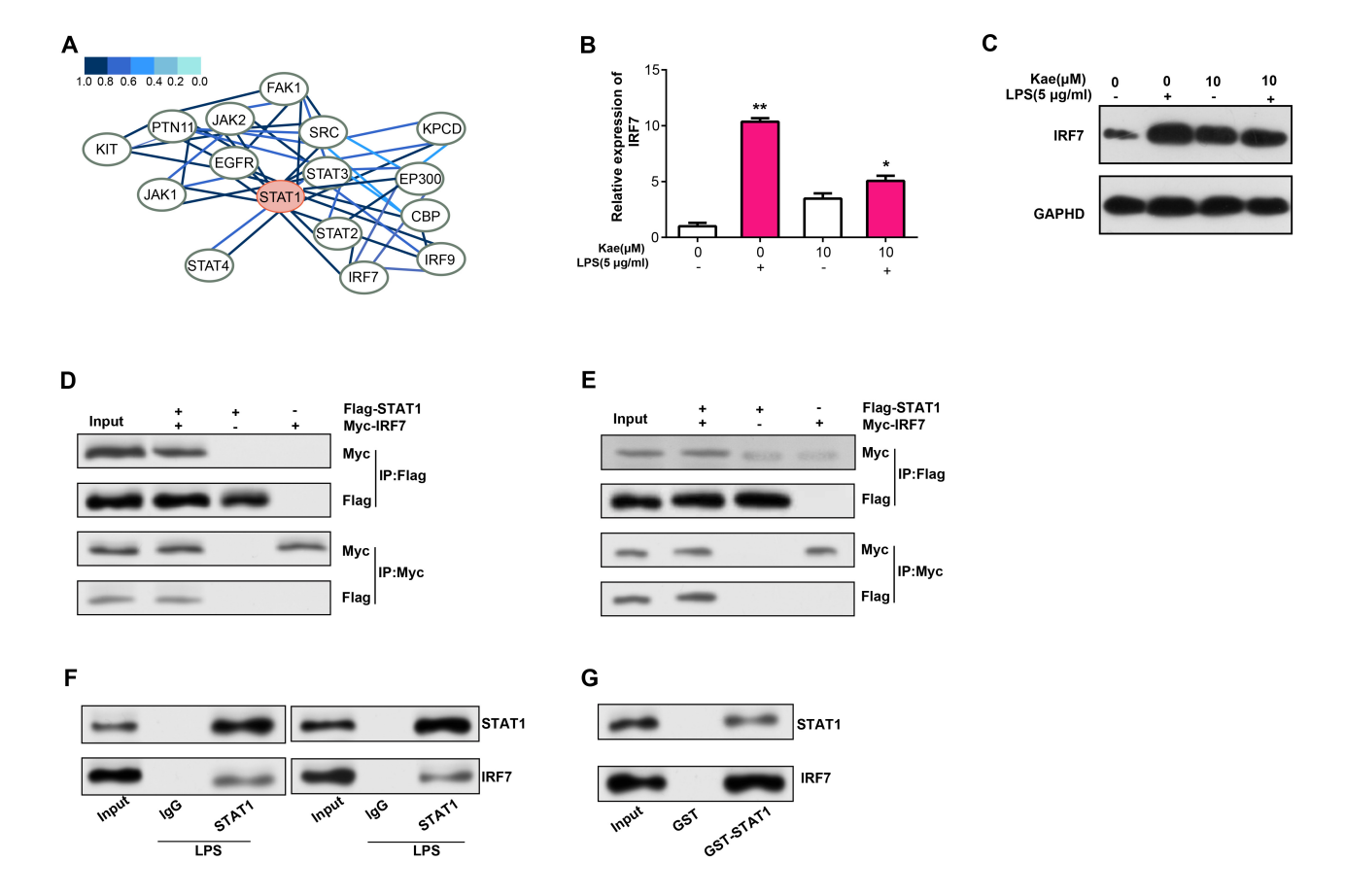


Fig. 8. Interaction analysis of STAT1 and IRF7 in LPS- and Kae-treated RPE cells. (A) PPI network depicting STAT1-interacting proteins based on the HitPredict database. (B) qRT-PCR analysis of IRF7 mRNA expression levels in RPE cells treated with LPS for 6 hours and pretreated with Kae for 24 hours. (C) WB analysis of IRF7 protein expression levels in RPE cells treated with LPS for 6 hours and pretreated with Kae for 24 hours. (D,E) Co-immunoprecipitation (Co-IP) assay demonstrating endogenous and exogenous interaction between STAT1 and IRF7. (F) Co-IP verifying the interaction between STAT1 and IRF7 in RPE cells. (G) Glutathione S-Transferase (GST) pull-down assay confirming the interaction between STAT1 and IRF7. *p < 0.05, *p < 0.01.

with genes in the key module, enriched in NOD-like receptor signaling pathway, Influenza A, Hepatitis C, NF-kappa B signaling pathway, etc. In the study by Michaelis M *et al.* [24], influenza A virus infection results in mild conjunctivitis, often involving retinal disease, possibly inflammation of the choriocapillaris, thus resulting in atrophy of the RPE. According to Luo S *et al.* [25], the C3a-C3aR and C5a-C5aR pathways might increase the viability and inflammatory response of RPE cells by blocking the NF-B signaling pathway. Furthermore, the investigation of Wang K further substantiates that the amyloid β -triggered activation of the NLRP3 inflammasome, a member of the NOD-like receptor family, is the culprit behind RPE dysfunction in AMD development [26].

Subsequently, we used the "ggvenn" package to perform the sub-networks of 370 intersecting genes based on the MCC and Degree algorithms, and identified 9 hub genes from them, namely *IFIT1*, *IFIT3*, *IRF7*, *ISG15*, *MX1*, *MX2*, *OASL*, *RSAD2*, *STAT1*. Then, our analysis indicated a generally high expression level of these genes in

the GSE30719 dataset's case group. The enrichment pathways of nine genes mainly included Lysine degradation, PRAR and JAK-STAT signaling, apoptosis, and RIG-I-like receptor signaling, among others. These genes have reportedly been linked to retinal illnesses in earlier studies. The interferon regulatory factor 7 (IRF7), a member of the interferon-regulated transcription factor family, participates in the transcriptional activation of cellular genes that are susceptible to viral induction [27]. Hooks JJ et al. [28] found that $IFN-\beta$ was produced in RPE cells infected with RNA virus, and the level of *IFN-\beta* continued to increase, which was related to the up-regulated IRF-7 level. In addition, the study of Wei TT et al. [29] found that IFN- γ participated in regulating the biological process of RPE cells by acting on genes, such as signal transducerand activator of transcription 1 (STAT1). However, the link between the remaining five genes and retinal diseases remains to be further studied. Based on the previous research and our findings, STAT1 was selected for the following study.



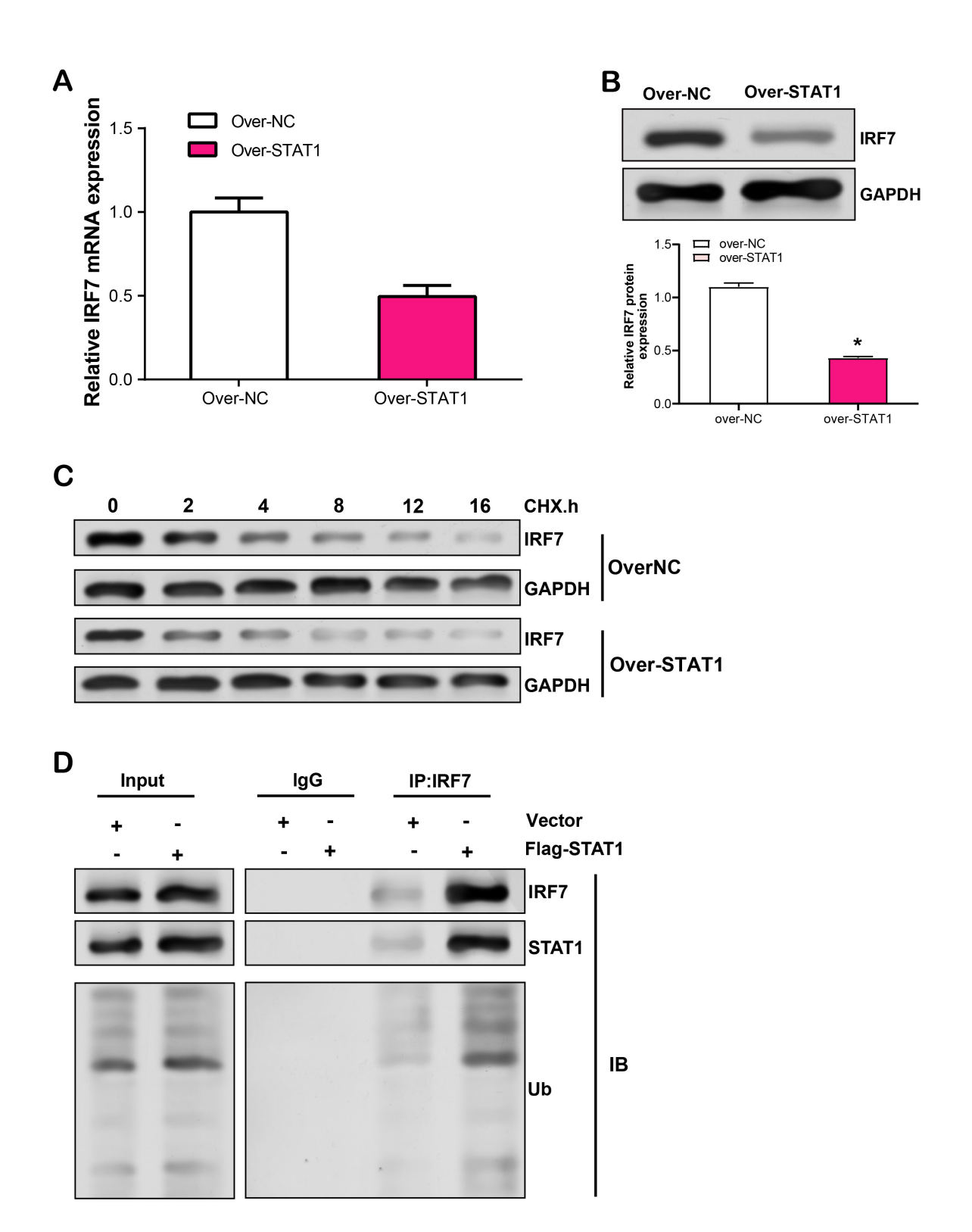


Fig. 9. Effects of LPS-induced STAT1 overexpression in RPE cells on IRF7 mRNA expression, protein stability, and ubiquitination. (A) qRT-PCR analysis of LPS-induced regulation of IRF7 mRNA expression level by overexpressed STAT1 in RPE cells. (B) WB analysis of LPS-induced regulation of IRF7 protein expression by overexpressed STATs in RPE cells. (C) WB detection of IRF7 protein stability in LPS-induced RPE cells treated with different durations of CHX in the control group and STAT1 overexpression group. (D) Co-IP analysis of the effect of STAT1 overexpression on LPS-induced IRF7 ubiquitination levels in RPE cells. *p < 0.05. NC, negative control; Ub, ubiquitination; IB, immunoblotting.

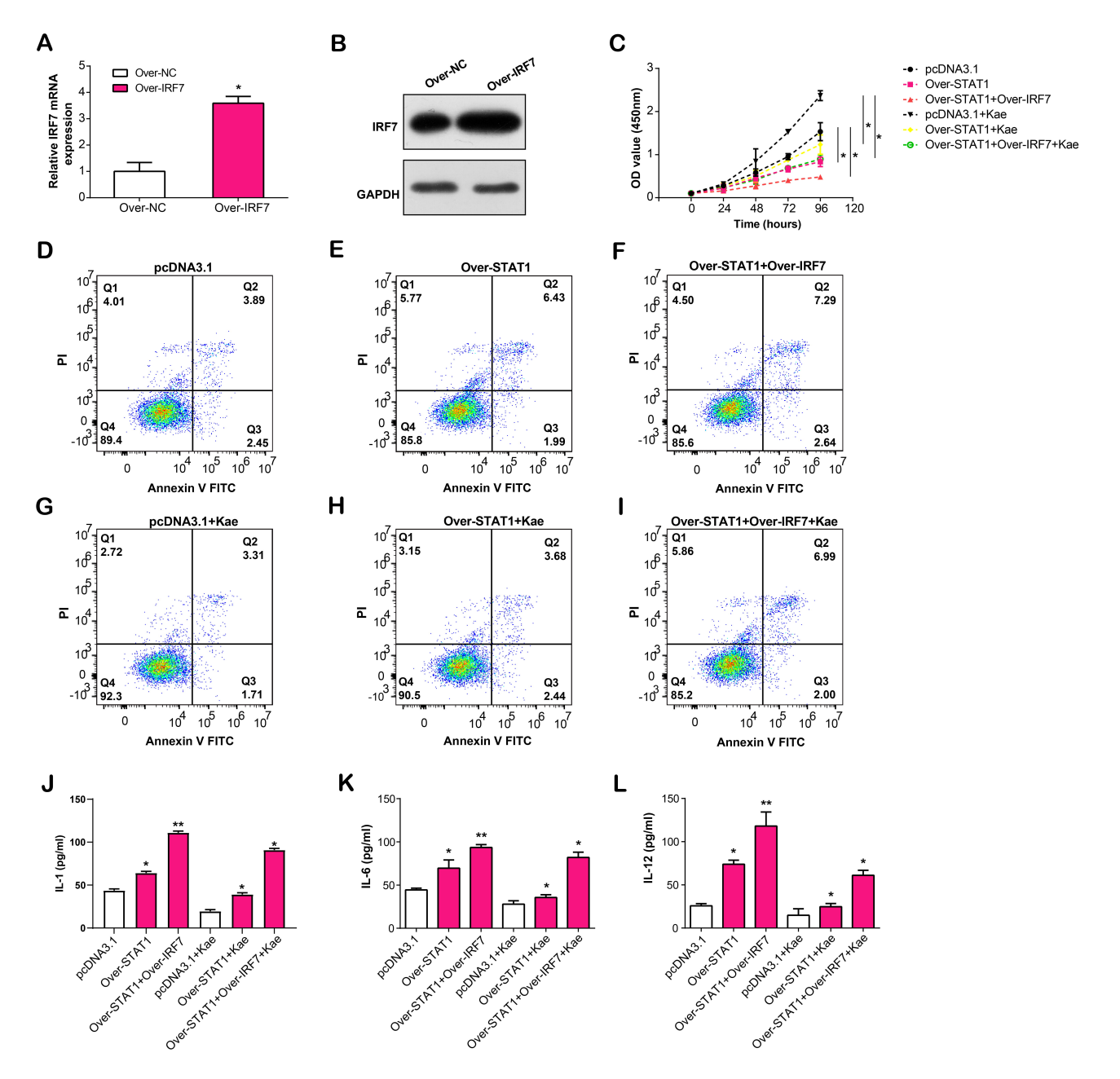


Fig. 10. Effects of STAT1/IRF7 overexpression and Kae treatment on proliferation, apoptosis, and cytokine secretion in LPS-induced RPE cells. (A,B) IRF7 overexpression efficiency in LPS-induced RPE cells using qRT-PCR and WB assays. (C) CCK-8 detects the proliferation activity of LPS-induced RPE cells after STAT1/IRF7 overexpression and Kae treatment. (D–I) Flow cytometry detection of the regulation of apoptosis by STAT1/IRF7 overexpression and Kae treatment in LPS-induced RPE cells. (J–L) ELSA detection of the secretion level of IL-1, IL-6 and IL-12 in the cell culture supernatant after STAT1/IRF7 overexpression and Kae treatment in LPS-induced RPE cells. **p < 0.05, **p < 0.01.

Gram-negative bacteria's outer membrane contains a significant amount of LPS, that may lead to inflammation and damage to RPE cells [30]. The use of LPS to stimulate RPE cells is a well-established model for investigating the underlying mechanisms of ocular inflammation and degeneration [31]. In previous studies, LPS has been shown to activate various signaling pathways, resulting in increased production of inflammatory mediators and ultimately lead-

ing to cell apoptosis [32]. Our research demonstrated that Kaempferol can attenuate LPS-induced RPE cell proliferation and reduce apoptosis in RPE cells. Numerous research examining the causes of RPE-related disorders have focused on the role of inflammatory cytokines, including as $IL-1\beta$, TNFR, IL-1, IL-6, and IL-12, in the pathogenesis of RPE cell damage [33]. Remarkably, our findings indicated that Kaempferol can reduce these inflammatory cytokines'



production in LPS-stimulated RPE cells. This research illuminates the therapeutic potential of Kae in reducing RPE injury and inflammation, which could lead to the creation of fresh approaches to the treatment of ocular conditions by RPE dysfunction.

STAT1 is a transcription factor involved in various cellular processes, including immune responses and apoptosis [34]. It has been implicated in several ocular disorders, including uveitis and age-related macular degeneration, where dysregulated STAT1 signaling contributes to disease progression. To elucidate the role of STAT1 in LPSinduced RPE cell injury, we performed expression analysis, confirming the downregulation of STAT1 expression in LPS-induced and Kae-treated RPE cells. Overexpression of STAT1 led to increased apoptosis rates and IL-1, IL-6 and IL-12 production levels in RPE cells. These findings suggested that overexpression of STAT1 promotes LPSinduced RPE cell apoptosis and exacerbates inflammation. Our study not only highlights the importance of STAT1 in LPS-induced RPE cell injury and inflammation, but also highlights the potential of Kae as a regulator of STAT1 expression and attenuation of LPS-induced RPE cell injury. This provided valuable insights into understanding the regulatory mechanism of STAT1 in RPE cells and developing novel therapeutic strategies targeting STAT1.

To further investigate the mechanisms of STAT1 in LPS-induced RPE cell injury, we utilized the HitPredict database to construct a PPI network for STAT1, which identified 15 potential interacting proteins. Among these candidates, we selected IRF7 for further analysis. IRF7 is a key transcription factor that controls inflammatory and immunological responses [35]. Previous researches have reported its function in various diseases, including autoimmune disease and viral infections, where dysregulation of IRF7 signaling contributes to pathogenesis [36]. In the article by Wu M et al. [37], IRF7 interacts with Smad3 in systemic sclerosis skin. Moreover, upregulation of IRF7 is also associated with excessive inflammation and fibrosis [37]. As a key regulator of systemic lupus erythematosus, IFN- α was confirmed to be regulated by IRF7 in the literature of Xu WD et al. [38], and the single nucleotide polymorphism of *IRF7* is also involved in the pathogenesis of systemic lupus erythematosus. In addition, Tucker MH et al. [39] also mentioned that IRF7 gene mutation is also associated with neonatal herpes simplex virus.

Our research showed that after LPS induction along Kae treatment, *IRF7* expression was downregulated within RPE cells. STAT1 and IRF7 interacted in co-IP as well as GST pull-down tests, suggesting their potential cooperative role in modulating LPS-induced RPE cell injury. Subsequent experiments showed that, in LPS-induced RPE cells, overexpression of *STAT1* did not affect the mRNA levels of *IRF7* but inhibited its protein expression. Furthermore, STAT1 was found to maintain IRF7 levels through deubiquitination. Finally, using CCK-8, flow cytometry,

and ELISA assays, we confirmed that Kae could inhibit LPS-induced RPE cell damage via the *STAT1/IRF7* axis. These findings highlighted the functional interplay between *STAT1* and *IRF7* in modulating LPS-induced RPE cell injury and Kae might be used as a form of therapy for RPE-related ocular disorders.

5. Conclusion

To sum up, we investigated possible therapeutic efficacy of Kae in RPE cells using *in vitro* tests. Our findings demonstrated that Kae not only attenuates LPS-induced RPE cell apoptosis but also reduces inflammatory cytokine production in LPS-induced RPE cells. Combined with the bioinformatics analysis, *STAT1* promotes RPE cell apoptosis and inflammation in response to LPS. Moreover, Kae appears to act in conjunction with the *STAT1/IRF7* axis in modulating LPS-induced RPE cell injury. Collectively, these results shed important light on Kae's protective effects on RPE cells and lay the foundation for further investigation into its potential applications in the treatment of RPE-related ocular diseases.

Availability of Data and Materials

The datasets used and/or analyzed during the current study are available from the corresponding author upon reasonable request.

Author Contributions

HZ and JJ designed the research study. HZ, YG and CL performed the research. YG and CG provided help and advice on the ELISA experiments. CL analyzed the data. All authors contributed to editorial changes in the manuscript. All authors read and approved the final manuscript. All authors have participated sufficiently in the work and agreed to be accountable for all aspects of the work.

Ethics Approval and Consent to Participate

Not applicable.

Acknowledgment

Not applicable.

Funding

This research received no external funding.

Conflict of Interest

The authors declare no conflict of interest.

References

[1] Massoumi H, Amin S, Soleimani M, Momenaei B, Ashraf MJ, Guaiquil VH, *et al.* Extracellular-Vesicle-Based Therapeutics in Neuro-Ophthalmic Disorders. International Journal of Molecular Sciences. 2023; 24: 9006.



- [2] Kleinlogel S, Vogl C, Jeschke M, Neef J, Moser T. Emerging Approaches for Restoration of Hearing and Vision. Physiological Reviews. 2020; 100: 1467–1525.
- [3] Fields MA, Del Priore LV, Adelman RA, Rizzolo LJ. Interactions of the choroid, Bruch's membrane, retinal pigment epithelium, and neurosensory retina collaborate to form the outer blood-retinal-barrier. Progress in Retinal and Eye Research. 2020; 76: 100803.
- [4] Barar J, Javadzadeh AR, Omidi Y. Ocular novel drug delivery: impacts of membranes and barriers. Expert Opinion on Drug Delivery. 2008; 5: 567–581.
- [5] Szatmári-Tóth M, Kristóf E, Veréb Z, Akhtar S, Facskó A, Fésüs L, et al. Clearance of autophagy-associated dying retinal pigment epithelial cells a possible source for inflammation in agerelated macular degeneration. Cell Death & Disease. 2016; 7: e2367.
- [6] Hinkle JW, Mahmoudzadeh R, Kuriyan AE. Cell-based therapies for retinal diseases: a review of clinical trials and direct to consumer "cell therapy" clinics. Stem Cell Research & Therapy. 2021; 12: 538.
- [7] Park SS, Bauer G, Abedi M, Pontow S, Panorgias A, Jonnal R, et al. Intravitreal autologous bone marrow CD34+ cell therapy for ischemic and degenerative retinal disorders: preliminary phase 1 clinical trial findings. Investigative Ophthalmology & Visual Science. 2014; 56: 81–89.
- [8] Kaarniranta K, Sinha D, Blasiak J, Kauppinen A, Veréb Z, Salminen A, et al. Autophagy and heterophagy dysregulation leads to retinal pigment epithelium dysfunction and development of age-related macular degeneration. Autophagy. 2013; 9: 973–984.
- [9] Fan W, Cheng Y, Wang B, Wang L, Zhou Q, Liu Y, et al. Metal-Organic Framework with Near-Infrared Luminescence for "Switch-on" Determination of Kaempferol and Quercetin by the Antenna Effect. Inorganic Chemistry. 2022; 61: 17185– 17195.
- [10] Shahbaz M, Imran M, Alsagaby SA, Naeem H, Al Abdulmonem W, Hussain M, et al. Anticancer, antioxidant, ameliorative and therapeutic properties of kaempferol. International Journal of Food Properties. 2023; 26: 1140–1166.
- [11] Kong L, Luo C, Li X, Zhou Y, He H. The anti-inflammatory effect of kaempferol on early atherosclerosis in high cholesterol fed rabbits. Lipids in Health and Disease. 2013; 12: 115.
- [12] Du W, An Y, He X, Zhang D, He W. Protection of Kaempferol on Oxidative Stress-Induced Retinal Pigment Epithelial Cell Damage. Oxidative Medicine and Cellular Longevity. 2018; 2018: 1610751.
- [13] Al Sabaani N. Kaempferol Protects Against Hydrogen Peroxide-Induced Retinal Pigment Epithelium Cell Inflammation and Apoptosis by Activation of SIRT1 and Inhibition of PARP1. Journal of Ocular Pharmacology and Therapeutics: the Official Journal of the Association for Ocular Pharmacology and Therapeutics. 2020; 36: 563–577.
- [14] Zou XL, Wang GF, Li DD, Chen JX, Zhang CL, Yu YZ, et al. Protection of tight junction between RPE cells with tissue factor targeting peptide. International Journal of Ophthalmology. 2018; 11: 1594–1599.
- [15] Yuan Z, Du W, He X, Zhang D, He W. Tribulus terrestris Ameliorates Oxidative Stress-Induced ARPE-19 Cell Injury through the PI3K/Akt-Nrf2 Signaling Pathway. Oxidative Medicine and Cellular Longevity. 2020; 2020: 7962393.
- [16] Iwakura Y, Nakae S, Saijo S, Ishigame H. The roles of IL-17A in inflammatory immune responses and host defense against pathogens. Immunological Reviews. 2008; 226: 57–79.
- [17] Kaur G, Singh NK. The Role of Inflammation in Retinal Neurodegeneration and Degenerative Diseases. International Journal of Molecular Sciences. 2021; 23: 386.

- [18] Avalle L, Pensa S, Regis G, Novelli F, Poli V. STAT1 and STAT3 in tumorigenesis: A matter of balance. JAK-STAT. 2012; 1: 65– 72.
- [19] Bhutto I, Lutty G. Understanding age-related macular degeneration (AMD): relationships between the photoreceptor/retinal pigment epithelium/Bruch's membrane/choriocapillaris complex. Molecular Aspects of Medicine. 2012; 33: 295–317.
- [20] Finnemann SC, Chang Y. Photoreceptor—RPE interactions. Visual Transduction and Non-Visual Light Perception. 2008; 67–86
- [21] Simó R, Villarroel M, Corraliza L, Hernández C, Garcia-Ramírez M. The retinal pigment epithelium: something more than a constituent of the blood-retinal barrier-implications for the pathogenesis of diabetic retinopathy. Journal of Biomedicine & Biotechnology. 2010; 2010: 190724.
- [22] Bertolotti E, Neri A, Camparini M, Macaluso C, Marigo V. Stem cells as source for retinal pigment epithelium transplantation. Progress in Retinal and Eye Research. 2014; 42: 130–144.
- [23] Zhang D, Robinson K, Washington I. C20D3-Vitamin A Prevents Retinal Pigment Epithelium Atrophic Changes in a Mouse Model. Translational Vision Science & Technology. 2021; 10: 8.
- [24] Michaelis M, Geiler J, Klassert D, Doerr HW, Cinatl J, Jr. Infection of human retinal pigment epithelial cells with influenza A viruses. Investigative Ophthalmology & Visual Science. 2009; 50: 5419–5425.
- [25] Luo S, Xu H, Gong X, Shen J, Chen X, Wu Z. The complement C3a-C3aR and C5a-C5aR pathways promote viability and inflammation of human retinal pigment epithelium cells by targeting NF-κB signaling. Experimental and Therapeutic Medicine. 2022; 24: 493.
- [26] Wang K, Yao Y, Zhu X, Zhang K, Zhou F, Zhu L. Amyloid β induces NLRP3 inflammasome activation in retinal pigment epithelial cells via NADPH oxidase- and mitochondria-dependent ROS production. Journal of Biochemical and Molecular Toxicology. 2017; 31.
- [27] Jefferies CA. Regulating IRFs in IFN Driven Disease. Frontiers in Immunology. 2019; 10: 325.
- [28] Hooks JJ, Nagineni CN, Hooper LC, Hayashi K, Detrick B. IFN-beta provides immuno-protection in the retina by inhibiting ICAM-1 and CXCL9 in retinal pigment epithelial cells. Journal of Immunology (Baltimore, Md.: 1950). 2008; 180: 3789–3796.
- [29] Wei TT, Zhang MY, Zheng XH, Xie TH, Wang W, Zou J, et al. Interferon-γ induces retinal pigment epithelial cell Ferroptosis by a JAK1-2/STAT1/SLC7A11 signaling pathway in Agerelated Macular Degeneration. The FEBS Journal. 2022; 289: 1968–1983.
- [30] Zhang D, Li X, Hu Y, Jiang H, Wu Y, Ding Y, et al. Tabersonine attenuates lipopolysaccharide-induced acute lung injury via suppressing TRAF6 ubiquitination. Biochemical Pharmacology. 2018; 154: 183–192.
- [31] Wang K, Zhu X, Zhang K, Yao Y, Zhuang M, Tan C, et al. Puerarin inhibits amyloid β-induced NLRP3 inflammasome activation in retinal pigment epithelial cells via suppressing ROS-dependent oxidative and endoplasmic reticulum stresses. Experimental Cell Research. 2017; 357: 335–340.
- [32] Sangaran PG, Ibrahim ZA, Chik Z, Mohamed Z, Ahmadiani A. LPS preconditioning attenuates apoptosis mechanism by inhibiting NF-κB and caspase-3 activity: TLR4 pre-activation in the signaling pathway of LPS-induced neuroprotection. Molecular neurobiology. 2021; 58: 2407–2422.
- [33] Ardeljan D, Chan CC. Aging is not a disease: distinguishing age-related macular degeneration from aging. Progress in Retinal and Eye Research. 2013; 37: 68–89.
- [34] Zhu L, Yang P, Zhao Y, Zhuang Z, Wang Z, Song R, et al. Single-Cell Sequencing of Peripheral Mononuclear Cells Reveals Dis-



- tinct Immune Response Landscapes of COVID-19 and Influenza Patients. Immunity. 2020; 53: 685–696.e3.
- [35] Cohen M, Matcovitch O, David E, Barnett-Itzhaki Z, Keren-Shaul H, Blecher-Gonen R, *et al.* Chronic exposure to $TGF\beta1$ regulates myeloid cell inflammatory response in an IRF7-dependent manner. The EMBO Journal. 2014; 33: 2906–2921.
- [36] Matta B, Song S, Li D, Barnes BJ. Interferon regulatory factor signaling in autoimmune disease. Cytokine. 2017; 98: 15–26.
- [37] Wu M, Skaug B, Bi X, Mills T, Salazar G, Zhou X, et al. Interferon regulatory factor 7 (IRF7) represents a link between in-
- flammation and fibrosis in the pathogenesis of systemic sclerosis. Annals of the Rheumatic Diseases. 2019; 78: 1583–1591.
- [38] Xu WD, Zhang YJ, Xu K, Zhai Y, Li BZ, Pan HF, *et al.* IRF7, a functional factor associates with systemic lupus erythematosus. Cytokine. 2012; 58: 317–320.
- [39] Tucker MH, Yu W, Menden H, Xia S, Schreck CF, Gibson M, et al. IRF7 and UNC93B1 variants in an infant with recurrent herpes simplex virus infection. The Journal of Clinical Investigation. 2023; 133: e154016.

